**Research Article**

**Open Access**

# MRI Characterizations of Region Specific White Matter Hyperintensities and Vertebral Artery Stenosis

**Liya Wang**[1,2], **Adrian Lam**[3], **John Oshinski**[1,2], **Xiaodong Zhong**[4], **Chad A Holder**[1], **Felicia Goldstein**[5], **Diana Ge**[2] and **Hui Mao**[1,2*]

[1]Department of Radiology and Imaging Sciences, Emory University School of Medicine, Atlanta, Georgia, USA

[2]Center for Systems Imaging, Emory University, Atlanta, Georgia, USA

[3]Department of Biomedical Engineering, Georgia Institute of Technology, Atlanta, Georgia, USA

[4]MR R&D Collaborations, Siemens Healthcare, Atlanta, Georgia, USA

[5]Department of Neurology, Emory University School of Medicine, Atlanta, Georgia, USA

**\*Corresponding author:** Hui Mao, PhD, Professor, Department of Radiology and Imaging Sciences, Emory University School of Medicine, Atlanta, Georgia, USA, Tel: 404-712-0357; E-mail: hmao@emory.edu

## Abstract

Cerebrovascular diseases cause brain degeneration and subsequent decline of cognitive functions. In this study, comprehensive magnetic resonance imaging approaches with both structural and blood flow imaging were used to characterize the white matter hyperintensity in the brain, cerebral blood flow, and obstruction of vertebral artery caused by stenosis in various cases of individuals with cerebral vascular and cardiovascular risks. It is demonstrated that vertebral artery stenosis characterized as vertebral artery narrowing and/or reduced blood flow velocity by MRI may be associated with the regional specific cerebral vascular comorbidities detected as white matter hyperintensity and reduction of cerebral blood flow. More specifically, unilateral vertebral artery stenosis led to asymmetric periventricular WMHs, while bilateral vertebral artery with lower blood flow led to symmetric periventricular WMHs. The comprehensive MRI protocol with functional and high resolution structural imaging sequences is capable of providing valuable information on blood flow supply in the vertebral artery and cerebrovascular ischemia in individuals having vertebral and cardiovascular abnormalities.

**Keywords:** Magnetic resonance imaging; Brain; White matter; Vertebral artery stenosis; Vascular disease; Blood flow rate

## Introduction

Increasing evidence has shown that cerebrovascular disease may contribute to the development of mild cognitive impairment (MCI) and dementia as well as the pathogenesis of Alzheimer's disease (AD) [1]. One indicator of cerebrovascular diseases is white matter hyperintensities (WMHs) observed by magnetic resonance imaging (MRI), which appear as high-signal foci within the subcortical white matter in T2-weighted spin-echo and fluid attenuated inversion recovery (FLAIR) images. Earlier reports have shown a greater severity of WMHs among patients with AD. Our recent work also suggests that WMH may be associated with the reduction of white matter integrity which is linked to the cognitive decline [2]. While WMHs are commonly found in patients with symptomatic cerebrovascular disease, they can also be seen in individuals with cardiovascular risk factors, such as hypertension and atherosclerosis. Therefore, it is important to examine the roles of multiple dimensions of vascular risk factors and how the progression of cerebrovascular disease facilitates the white matter degeneration and cognitive decline. One specific interest is to examine the association between cerebral vascular abnormalities and carotid and/or vertebral artery stenosis. Carotid and vertebral arteries channel oxygenated blood to the posterior part of the brain. Atherosclerosis, or hardening of the arteries, mostly due to fatty substance deposition and plaque formation, can lead to narrowing of the blood vessels. Several studies have assessed the relationship

between WMHs and the risk of stroke, dementia, and carotid artery diseases [3-5]. However, the optimal management of vertebral artery stenosis has received limited attention, and is not well understood [6]. Unlike carotid diseases, the prognosis of symptomatic vertebral artery stenosis is also largely unknown [7]. This partly reflects difficulties in imaging of extracranial vertebral artery adequately.

MRI is sensitive for detecting anatomic and pathological abnormalities with exquisite soft tissue contrast and high spatial resolution. In addition to characterization of cerebral tissue integrity and infarcts, such as WMHs, MRI also offers capabilities to examine vascular structure and function. For example, relative cerebral blood flow (relCBF) and volume can be measured using Arterial Spin Labeling (ASL) perfusion imaging without administration of exogenous contrast agents. In ASL a radiofrequency pulse is used to tag the inflow blood in a section of the carotid artery and subsequently measure the amount of tagged blood in the brain [8]. By applying velocity-encoding gradients, Phase Contrast Magnetic Resonance Imaging (PCMR) acquires the phase information from the images to calculate the velocity of the blood flow in arterial vessels [9-10]. Furthermore, Magnetic Resonance Angiography (MRA) techniques can generate blood vessel images for identification of stenosis, occlusions, aneurysms or other vasculature obstructions from high-resolution images [11,12]. Therefore, it is possible to study cerebral vascular abnormalities and function as well as obstruction of proximal extracranial vertebral artery with these non-invasive and clinically feasible neuroimaging methods in the same imaging session.

Here we present various cases of MRI examinations of individuals with cerebral vascular and cardiovascular risks to demonstrate the

association between extracranial vertebral artery stenosis evidenced by obstructed artery and blood flow velocity and cerebral vascular comorbidities, particularly WMHs and reduction of cerebral blood flow in specific brain regions.

## Material and Methods

### Subjects

This study was approved by the local Institutional Review Board for the human subject research. Written consents were obtained from fifteen consecutive participants (3 men, 12 women; average age of 60.1 ± 9.1 years old) before the study. Based on vertebral artery stenosis and the specific location of WMHs, 15 subjects were grouped into: 1) left vertebral artery stenosis with bilateral asymmetric periventricular WMHs (n=4), 2) right vertebral artery stenosis with bilateral asymmetric periventricular WMHs (n=7), and 3) bilateral vertebral arteries stenosis with similar caliber with bilateral symmetric periventricular WMHs (n=4). All participants did not have histories or findings suggestive of stroke as determined by reviewing their medical records and a neurologic exam.

### MRI acquisition and data analysis

The MRI protocol included whole-brain T2 weighted fast spin echo imaging, FLAIR imaging, ASL perfusion imaging, PCMR, and MRA imaging. All images were acquired on a whole body 3T MRI scanner (Siemens Tim Trio, Siemens Healthcare, Erlangen, Germany) using a standard 12-channel head coil and a four-element phased array carotid coil (Machnet, Maastricht, The Netherlands) when needed.

T2 weighted fast spin echo images (TR=4900 ms and TE=110 ms) were collected with 60 slices, 2 mm thickness and no gap, followed by a FLAIR sequence, with TR=6000 ms and TE=81 ms with 27 slices and 4 mm slice thickness to detect WMHs. A 3D TOF sequence was then performed to provide bright blood signal, 60-slice region of interest (ROI) centered at the carotid bifurcation to obtain high signal-to-noise (SNR), high resolution images for evaluation of the vessel lumen.

| Subject | Age | Sex | Weight (kg) | PVWMHs | RVA (mm) | LVA (mm) | rCBF |
|---|---|---|---|---|---|---|---|
| 1 | 68 | F | 57.2 | (++) | 3.8 | 4.9 | reduction |
| 2 | 64 | F | 66.1 | (+) | 5.7 | 3.2 | reduction |
| 3 | 58 | F | 95.8 | (+) | 4.5 | 5.2 | reduction |
| 4 | 66 | M | 68 | (++)* | 2.4 | 4.6 | reduction |
| 5 | 55 | F | 66.7 | (++) | 3.2 | 5.7 | reduction |
| 6 | 66 | F | 106.1 | (+) | 3.6 | 4.8 | reduction |
| 7 | 62 | M | 71.3 | (+) | 5.2 | 4.9 | reduction |
| 8 | 58 | F | 77.1 | (+) | 5.3 | 5.1 | N/A |
| 9 | 62 | F | 76.2 | (+)* | 5.1 | 4.1 | N/A |
| 10 | 37 | F | 90.7 | (+) | 4.9 | 4.7 | reduction |
| 11 | 50 | F | 82.1 | (+) | 5.2 | 3.7 | reduction |
| 12 | 75 | F | 90.7 | (++) | 3.3 | 4.7 | reduction |
| 13 | 68 | F | 120.2 | (++)* | 3.9 | 4.8 | N/A |
| 14 | 55 | M | 117 | (+) | 5.1 | 4.3 | N/A |
| 15 | 58 | F | 93.4 | (+) | 4.9 | 5.2 | N/A |

Notes: PVWMHs indicated periventricular WMHs in the occipital horns with minor WMHs marking as (+) and severe WMHs marking as (++). * indicated periventricular WMHs were not only in the occipital horns. RVA/LVA means inside diameter in the right/left vertebral artery. N/A indicated not available.

Table 1: Subjects demographics and specific findings

PCMR images encoded for through-plane blood velocity were acquired at the inlet of the common carotid artery (CCA) at the same location as the proximal slice of the 3D-TOF image stack. The imaging parameters included 30 cardiac phases, pixel size=1.1X1.1 mm2, slice thickness=6 mm, and VENC=100 cm/s. The proximal extracranial vertebral arteries and the internal carotid arteries were processed offline using Segment (Medviso AB, Lund, Sweden) [13]. Vessel borders were drawn on magnitude images and contours were transferred directly to the corresponding phase images. Pixel-by-pixel velocity values were then integrated over the region of interest (ROI) to obtain flow rates for each time point. Net flow over the cardiac cycle was quantified from these time dependent flow rate data.

ASL images were acquired using single-shot echo-planar imaging (EPI) [14,15], consisting of five 8-mm-thick slices with 2-mm gaps with an in-plane resolution of 2.3X2.3 mm2 oriented 10° up from the anterior-posterior commissural line and covered the volume above this line. Other acquisition parameters were as follows: TR/TE=2500/15 ms, TI1 (start time of the periodic saturation pulses)=700 ms, TI2 (time from labeling pulse to the excitation pulse)=1800 ms,

saturation stop time=1600 ms, and flow limit=100 cm/s. Relative cerebral blood flow (relCBF) was generated inline on the scanner by the ASL sequence for assessing possible cerebral hypoperfusion [16,17].

## Results

The demographics and specific findings of all subjects are summarized in Table 1. Unfortunately, no diagnostic records were collected, therefore the pathology information of the patients were unknown.

### Unilateral vertebral artery stenosis led to asymmetric periventricular WMHs
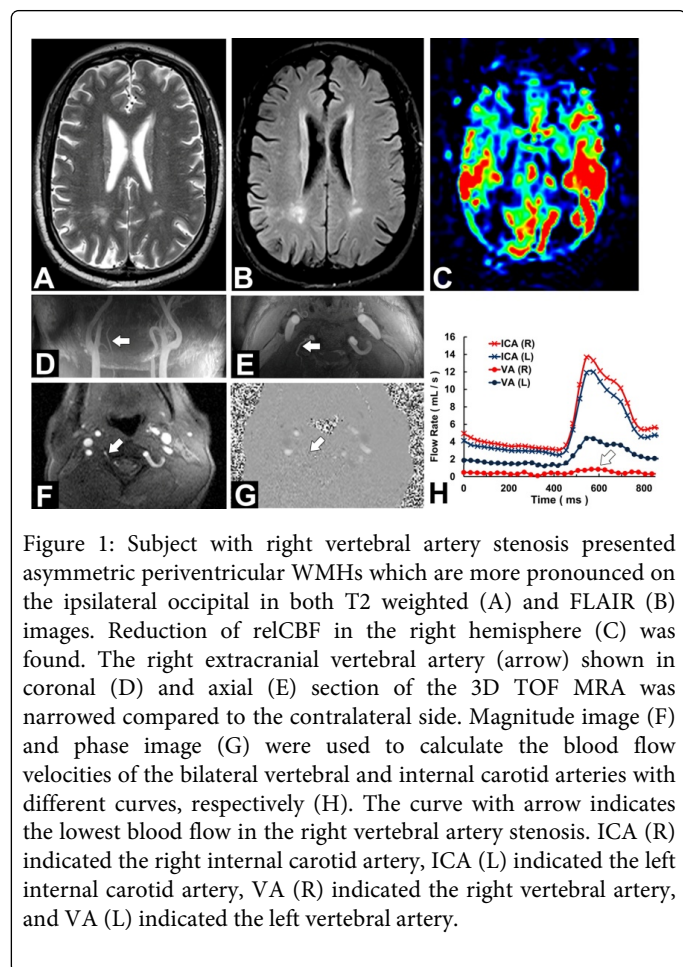


Figure 1: Subject with right vertebral artery stenosis presented asymmetric periventricular WMHs which are more pronounced on the ipsilateral occipital in both T2 weighted (A) and FLAIR (B) images. Reduction of relCBF in the right hemisphere (C) was found. The right extracranial vertebral artery (arrow) shown in coronal (D) and axial (E) section of the 3D TOF MRA was narrowed compared to the contralateral side. Magnitude image (F) and phase image (G) were used to calculate the blood flow velocities of the bilateral vertebral and internal carotid arteries with different curves, respectively (H). The curve with arrow indicates the lowest blood flow in the right vertebral artery stenosis. ICA (R) indicated the right internal carotid artery, ICA (L) indicated the left internal carotid artery, VA (R) indicated the right vertebral artery, and VA (L) indicated the left vertebral artery.

Among 15 cases collected in this study, seven presented right vertebral artery stenosis with asymmetric periventricular WMHs in the occipital horns, which was more pronounced in the ipsilateral occipital region. These WMHs observed in both T2 weighted (Figure 1A) and FLAIR (Figure 1B) images appear as a hyperintense band with variable thickness located along the dorsolateral angles of the ventricles close to the ependymal surface. The reduction of relCBF was found in the bilateral occipital lobes, but predominantly in the right occipital lobe, as shown in Figure 1C, which was consistent with the significant narrowing of right extracranial vertebral artery (>80%) observed in 3D TOF MRA (Figure 1D). However, the sizes of the bilateral carotid arteries were similar as shown in Figure 1D and 1E.

The internal diameter of the right vertebral artery was measured at 2.4 mm. In comparison, the internal diameters of the left vertebral artery, right carotid artery, and left carotid artery were 4.6 mm, 7.2 mm, and 8.4 mm, respectively (Figure 1F). PCMR confirmed there was decreased blood flow velocity in the right vertebral artery (arrow, Figure 1G), comparing to the left one (Figure 1H).
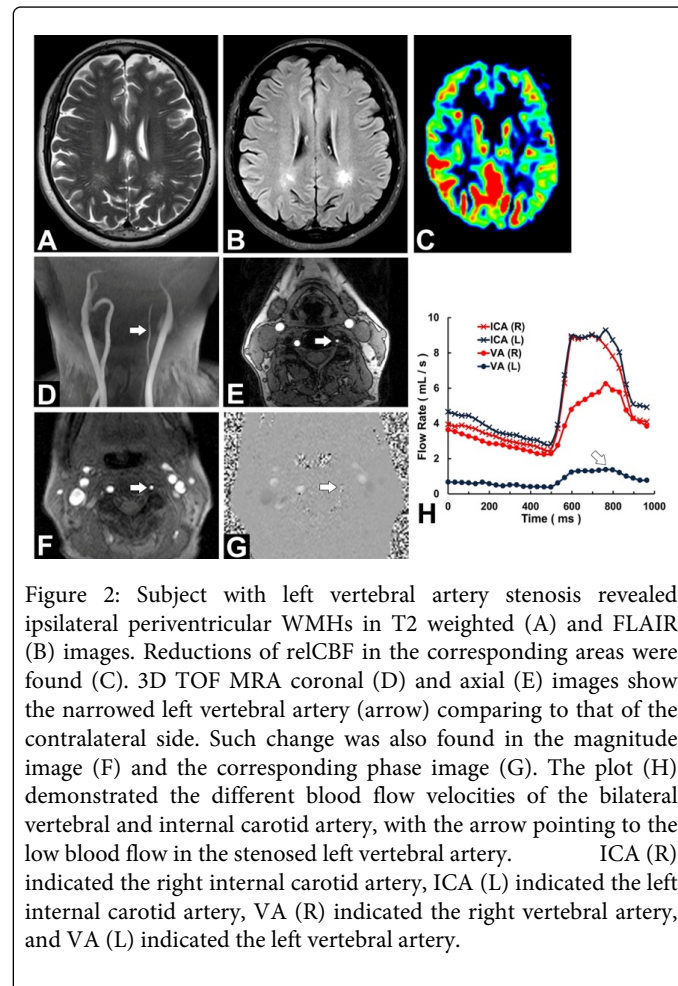


Figure 2: Subject with left vertebral artery stenosis revealed ipsilateral periventricular WMHs in T2 weighted (A) and FLAIR (B) images. Reductions of relCBF in the corresponding areas were found (C). 3D TOF MRA coronal (D) and axial (E) images show the narrowed left vertebral artery (arrow) comparing to that of the contralateral side. Such change was also found in the magnitude image (F) and the corresponding phase image (G). The plot (H) demonstrated the different blood flow velocities of the bilateral vertebral and internal carotid artery, with the arrow pointing to the low blood flow in the stenosed left vertebral artery. ICA (R) indicated the right internal carotid artery, ICA (L) indicated the left internal carotid artery, VA (R) indicated the right vertebral artery, and VA (L) indicated the left vertebral artery.

Figure 2 presents another example about unilateral vertebral artery stenosis leading to ipsilateral periventricular WMHs. In four cases with left vertebral artery stenosis, they all exhibited unilateral vertebral artery stenosis that can be associated with bilateral asymmetrical periventricular WMHs, which was more pronounced in the left occipital horns in T2 weighted imaging (Figure 2A). Furthermore, the FLAIR image revealed such asymmetrical appearances of WMHs in the occipital horn along with punctuate and confluent lesion adjacent to the occipital horn of the anterior periventricular areas (Figure 2B). In this case, the FLAIR image was found to have a better sensitivity to WMHs than T2 weighted imaging, especially for those at periventricular locations. Besides identifying infarcts from structural imaging, relCBF map calculated from the ASL images demonstrated decreased relCBF in the left rostral occipital cortex and parietal cortex, including angular gyrus, supramarginal gyrus, and postcentral gyrus (Figure 2C). MRA of head and neck generated from 3D TOF MRI (Figures 2D and 2E) showed marked narrowing of the left proximal extracranial vertebral artery (>70%) with the internal diameter measured at 3.2 mm, comparing to 5.7 mm diameter of the right

vertebral artery. The diameters of carotid arteries were 6.5 mm (left) and 7.7 mm (right), respectively (Figure 2F). The flow velocity calculation based on PCMR (Figure 2G) suggested that there was a decrease in blood flow rate in the left proximal extracranial vertebral artery, but not in the right extracranial vertebral artery and bilateral carotid artery as shown in Figure 2H. These findings suggest that periventricular WMHs in the occipital horn might be caused by ipsilateral vertebral artery stenosis.

## Bilateral vertebral artery with lower blood flow led to symmetric periventricular WMHs
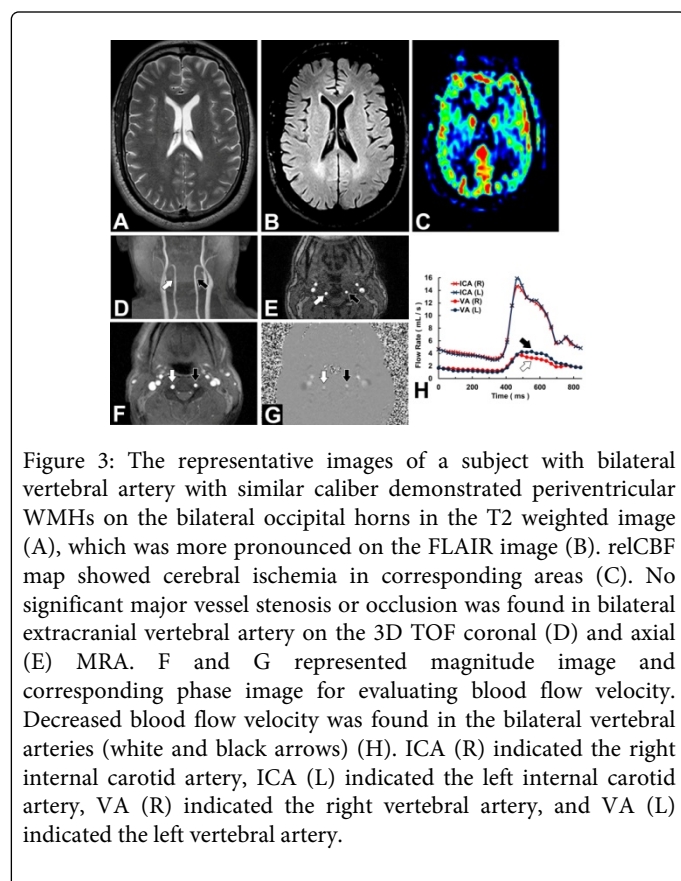


Figure 3: The representative images of a subject with bilateral vertebral artery with similar caliber demonstrated periventricular WMHs on the bilateral occipital horns in the T2 weighted image (A), which was more pronounced on the FLAIR image (B). relCBF map showed cerebral ischemia in corresponding areas (C). No significant major vessel stenosis or occlusion was found in bilateral extracranial vertebral artery on the 3D TOF coronal (D) and axial (E) MRA. F and G represented magnitude image and corresponding phase image for evaluating blood flow velocity. Decreased blood flow velocity was found in the bilateral vertebral arteries (white and black arrows) (H). ICA (R) indicated the right internal carotid artery, ICA (L) indicated the left internal carotid artery, VA (R) indicated the right vertebral artery, and VA (L) indicated the left vertebral artery.

We also found four cases that showed symmetrical minor WMHs in the areas of bilateral periventricular occipital horns seen in T2 weighted images (Figure 3A), which were more pronounced in the FLAIR image (Figure 3B). The lesions mostly appeared as punctate WMHs adjacent to the bilateral occipital horns. No juxtacortical or posterior fossa lesions were observed. The relCBF map revealed decreased CBF in bilateral occipital regions (Figure 3C), although no significant major vessel stenosis or occlusion was observed in bilateral proximal extracranial vertebral artery (Figure 3D and 3E). The internal diameter of the right vertebral artery, left vertebral artery, right carotid artery, and left carotid artery were 4.9 mm, 5.2 mm, 6.7 mm and 6.4 mm, respectively (Figure 3F). However, blood flow velocity appeared to be slow in the bilateral proximal extracranial vertebral artery detected in PCMR (Figure 3G). The relevant changes were plotted in Figure 3H. These findings suggest that low blood flow velocity might contribute to the cause of WMHs in the periventricular occipital horns even though no apparent bilateral extracranial vertebral artery narrowing was observed. From the neuroimaging technique

perspective, PCMR with information on flow velocity seems to provide more sensitive and specific detection of vasculature abnormalities in the extracranial vertebral arteries than 3D TOF MRI due to its quantitative capability.

## Discussion

WMHs commonly seen on MR images are related to various neurological disorders, including cerebrovascular diseases, cardiovascular diseases, dementia, and psychiatric disorders[18]. Although the pathogenic mechanisms of periventricular WMHs are still under investigation [19], it has been increasingly believed that ischemic cerebrovascular disease, not only from carotid artery disease, but also due to vertebral artery stenosis, is one of the common causes of posterior circulation ischemia and leads to cerebral WMHs.

Extracranial vertebral artery is affected by several pathological processes. Stenosis of the vertebral artery can occur in either its extra- or intracranial portions, and may account for up to 20% of posterior circulation ischemic strokes [20-23]. Some studies have reported that atherosclerotic disease at the first part of the vertebral artery was commonly associated with similar disease in the internal carotid artery [24,25] because both vertebral arteries feed into one basilar artery. However, none of the isolated vertebral artery stenosis develops into posterior circulation infarction [26]. The findings of this study demonstrated that the vertebral artery obstruction due to either unilateral or bilateral stenosis may cause reduction of cerebral blood supply and subsequent periventricular white matter damage in the occipital area. More specifically, we found unilateral vertebral artery stenosis without bilateral carotid artery ischemia contributed to WMHs in either ipsilateral or bi-periventricular occipital horns (Figures 1 and 2). On the other hand, symmetric WMHs could be found in bi-periventricular occipital horns in FLAIR or T2 weighted imaging (Figure 3), when extracranial vertebral artery had symmetric narrowing but without carotid artery blood flow reduction.

In addition to report the findings of possible association between extracranial vertebral artery and cerebral white matter ischemic damage, we presented a MRI protocol combining T2 weighted imaging, FLAIR, 3D TOF MRA, and PCMR to characterize extracranial vertebral artery stenosis, vertebral artery the blood flow velocity change and related structural and vascular abnormalties in the brain. This neuroimaging protocol provides comprehensive and multi-dimensional assessment of "function-structure" relationships of the brain and vasculature. It is translational and clinically feasible when there is a need for obtaining a systematic characterization of cerebral vascular diseases.

We recognize that the current study is limited by the sample size, making it difficult to perform typical statistical analysis. A quantitative correlation between the degree of WMHs and the severity of extracranial vertebral artery stenosis would greatly enhance and validate the preliminary findings presented here. Thus, the results from this study will need to be further validated with more extensive and quantitative investigations in the future.

## Conclusions

We demonstrated that vertebral artery stenosis characterized as vertebral artery narrowing and/or reduced blood flow velocity by MRI may be associated with the regional specific cerebral vascular comorbidities detected as white matter hyperintensity and reduction of cerebral blood flow. This comprehensive MRI protocol with

functional and high resolution structural imaging sequences is capable of providing valuable information on blood flow supply in the vertebral artery and cerebrovascular ischemia in individuals having vertebral and cardiovascular abnormalities.

## Acknowledgement

## References

1. Launer LJ (2004) Epidemiology of white matter lesions. Top Magn Reson Imaging 15: 365-367.

2. Wang L, Goldstein FC, Levey AI, Lah JJ, Meltzer CC, et al. (2011) White matter hyperintensities and changes in white matter integrity in patients with Alzheimer's disease. Neuroradiology 53: 373-381.

3. Altaf N, Morgan PS, Moody A, MacSweeney ST, Gladman JR, et al. (2008) Brain white matter hyperintensities are associated with carotid intraplaque hemorrhage. Radiology 248: 202-209.

4. Murray AD, Staff RT, Shenkin SD, Deary IJ, Starr JM, et al. (2005) Brain white matter hyperintensities: relative importance of vascular risk factors in nondemented elderly people. Radiology 237: 251-257.

5. Pantoni L, Garcia JH (1997) Pathogenesis of leukoaraiosis: a review. Stroke 28: 652-659.

6. Scheltens P, Barkhof F, Leys D, Pruvo JP, Nauta JJ, et al. (1993) A semiquantative rating scale for the assessment of signal hyperintensities on magnetic resonance imaging. J Neurol Sci 114: 7-12.

7. Cloud GC, Markus HS (2003) Diagnosis and management of vertebral artery stenosis. QJM 96: 27-54.

8. Bastos-Leite AJ, Kuijer JP, Rombouts SA, Sanz-Arigita E, van Straaten EC, et al. (2008) Cerebral blood flow by using pulsed arterial spin-labeling in elderly subjects with white matter hyperintensities. AJNR Am J Neuroradiol 29: 1296-1301.

9. Moran PR (1982) A flow velocity zeugmatographic interlace for NMR imaging in humans. Magn Reson Imaging 1: 197-203.

10. Naidich TP, Altman NR, Gonzalez-Arias SM (1993) Phase contrast cine magnetic resonance imaging: normal cerebrospinal fluid oscillation and applications to hydrocephalus. Neurosurg Clin N Am 4: 677-705.

11. Lin W, Tkach JA, Haacke EM, Masaryk TJ (1993) Intracranial MR angiography: application of magnetization transfer contrast and fat saturation to short gradient-echo, velocity-compensated sequences. Radiology 186: 753-761.

12. Masaryk TJ, Modic MT, Ross JS, Ruggieri PM, Laub GA, et al. (1989) Intracranial circulation: preliminary clinical results with three-dimensional (volume) MR angiography. Radiology 171: 793-799.

13. Soneson H, Ubachs JF, Ugander M, Arheden H, Heiberg E (2009) An improved method for automatic segmentation of the left ventricle in myocardial perfusion SPECT. J Nucl Med 50: 205-213.

14. Du AT, Jahng GH, Hayasaka S, Kramer JH, Rosen HJ, et al. (2006) Hypoperfusion in frontotemporal dementia and Alzheimer disease by arterial spin labeling MRI. Neurology 67: 1215-1220.

15. Jahng GH, Zhu XP, Matson GB, Weiner MW, Schuff N (2003) Improved perfusion-weighted MRI by a novel double inversion with proximal labeling of both tagged and control acquisitions. Magn Reson Med 49: 307-314.

16. Asllani I, Habeck C, Scarmeas N, Borogovac A, Brown TR, et al. (2008) Multivariate and univariate analysis of continuous arterial spin labeling perfusion MRI in Alzheimer's disease. J Cereb Blood Flow Metab 28: 725-736.

17. Brickman AM, Zahra A, Muraskin J, Steffener J, Holland CM, et al. (2009) Reduction in cerebral blood flow in areas appearing as white matter hyperintensities on magnetic resonance imaging. Psychiatry Res 172: 117-120.

18. Kim KW, MacFall JR, Payne ME (2008) Classification of white matter lesions on magnetic resonance imaging in elderly persons. Biol Psychiatry 64: 273-280.

19. Román GC, Erkinjuntti T, Wallin A, Pantoni L, Chui HC (2002) Subcortical ischaemic vascular dementia. Lancet Neurol 1: 426-436.

20. Brant-Zawadzki M, Fein G, Van Dyke C, Kiernan R, Davenport L, et al. (1985) MR imaging of the aging brain: patchy white-matter lesions and dementia. AJNR Am J Neuroradiol 6: 675-682.

21. Fazekas F, Chawluk JB, Alavi A, Hurtig HI, Zimmerman RA (1987) MR signal abnormalities at 1.5 T in Alzheimer's dementia and normal aging. AJR Am J Roentgenol 149: 351-356.

22. Koroshetz WJ, Ropper AH (1987) Artery-to-artery embolism causing stroke in the posterior circulation. Neurology 37: 292-295.

23. Longstreth WT Jr, Manolio TA, Arnold A, Burke GL, Bryan N, et al. (1996) Clinical correlates of white matter findings on cranial magnetic resonance imaging of 3301 elderly people. The Cardiovascular Health Study. Stroke 27: 1274-1282.

24. Castaigne P, Lhermitte F, Gautier JC, Escourolle R, Derouesne C, et al. (1973) Arterial occlusions in the vertebro-basilar system. A study of 44 patients with post-mortem data. Brain 96: 133-154.

25. Hutchinson EC, Yates PO (1956) The cervical portion of the vertebral artery; a clinico-pathological study. Brain 79: 319-331.

26. Moufarrij NA, Little JR, Furlan AJ, Williams G, Marzewski DJ (1984) Vertebral artery stenosis: long-term follow-up. Stroke 15: 260-263.